Excess sound absorption at normal incidence by two microperforated panel absorbers with different impedance

Yairi, Motoki
Sakagami, Kimihiro
Takebayashi, Kenichi
Morimoto, Masayuki

(Citation)
Acoustical Science and Technology,32(5):194-200

(Issue Date)
2011-09-01

(Resource Type)
journal article

(Version)
Version of Record

(URL)
https://hdl.handle.net/20.500.14094/90001613

Acoust. Sci. & Tech. **32**, 5 (2011)

PAPER

Excess sound absorption at normal incidence by two microperforated panel absorbers with different impedance

Motoki Yairi[1,*], Kimihiro Sakagami[2], Kenichi Takebayashi[1] and Masayuki Morimoto[2]

[1]*Kajima Technical Research Institute, Tobitakyu, Chofu, 182–0036 Japan*
[2]*Environmental Acoustics Laboratory, Graduate School of Engineering, Kobe University, Rokko, Nada, Kobe, 657–850 Japan*

(*Received 12 November 2010, Accepted for publication 31 March 2011*)

Abstract: A microperforated panel (MPP) absorber is known to be one of the most promising alternatives of the next-generation sound absorbers. However, its absorption frequency range is limited to around two octaves because its absorption solely depends on the Helmholtz resonance mechanism. Therefore, the authors have proposed a combination of two different MPP absorbers in parallel, and revealed its potential for achieving a broader absorption frequency range in terms of excess attenuation. In this study, by the hybrid method of BEM and a mode expansion method, the authors investigate the relationship between the excess attenuation caused by the impedance discontinuity at the boundary of the two different MPPs and the sound absorption coefficient derived using the electro acoustical equivalent circuit model. Measurements of the normal incidence absorption coefficients are carried out to validate the equivalent circuit model, and in the experiments, the configuration of the cavity to realize the parallel arrangements for achieving wideband sound absorption is also discussed referring to the experimental results.

Keywords: Excess sound absorption, Microperforated panel, Parallel Arrangement, Wideband sound absorption, Electro-acoustical equivalent circuit model

PACS number: 43.55.Ev [doi:10.1250/ast.32.194]

1. INTRODUCTION

Microperforated panel (MPP) sound absorbers are promising as a basis for the next generation of sound absorbing materials [1–3]. MPPs are usually placed in front of a rigid back wall with an air cavity, and Helmholtz resonators are formed with its perforation and the back cavity. This offers high sound absorption performance in relatively a wide frequency range from mid- to high frequencies. Since Maa's pioneering works [1], many studies have been conducted on the application of MPPs for various purposes including attenuating noise in small rooms [4,5], duct silencing systems [6], acoustic window systems [7], and noise barriers [8].

The absorption frequency range of the MPP sound absorbers is certainly wider than those of resonance-type absorbers. However, it is limited to around two octaves because its absorption solely depends on the Helmholtz resonance mechanism. Therefore, in efforts to widen the absorption frequency range, many studies have been performed. The multiple-leaf MPP absorbers were first proposed by Maa [1,2], and a couple of studies have followed [9,10]. These absorbers are intended to produce a double resonator with two resonance frequencies. For this purpose, in multiple-leaf MPPs, the leaves should be arranged in a series.

In order to widen the absorption frequency range, a double-leaf MPP without a back wall (DLMPP) was also proposed [11,12]. This structure acts as a Helmholtz-type absorber at mid- to high frequencies, as well as a permeable-type absorber with acoustical resistance to absorb sound energy at low frequencies, and consequently, the absorption characteristics cover a broader absorption frequency range.

On the other hand, the authors found that a honeycomb in the cavity can improve the sound absorption performance of a MPP absorber [13,14]. This structure was originally intended to make the MPPs stiff enough for room

*e-mail: yairi@kajima.com

interior surfaces. However, the honeycomb can realize the local reacting condition in the cavity, which makes the absorption characteristics similar to those for normal incidence. Thus, the honeycomb is not only useful for strengthening thin MPPs but also effective for enhancing the resonance absorption peak and extending it to lower frequencies.

As mentioned above, in most previous studies, MPPs were arranged in series along the direction of the incident sound waves. This arrangement necessarily increases the total depth of the absorbers, making them unsuitable for room interior surfaces in buildings. Therefore, from a different point of view from the previous studies, the authors proposed a combination of two different MPP absorbers not arranged in series but in parallel, and revealed its potential for achieving a broader absorption frequency range in terms of excess attenuation [15].

In this study, the authors investigate the relationship between the excess attenuation caused by the impedance discontinuity of MPP absorbers and the two types of sound absorption coefficients: one is the statistical average of the sound absorption coefficient and the other is that derived using the electro acoustical equivalent circuit. Next, the normal incidence absorption coefficients are measured in an impedance tube to validate the equivalent circuit model. In the experiments, the configuration of the cavity to realize the parallel arrangements for achieving a wideband sound absorption is also discussed referring to the experimental results.

2. THEORETICAL CONSIDERATIONS

2.1. Hybrid Method of BEM and Mode Expansion Method

In our previous study [15], the sound absorption coefficient considering the excess attenuation was obtained using a theoretical expression [16]. In the present study, however, we use the hybrid method of BEM and a mode expansion method [17], because the structures can be extended to any other shape without any fundamental changes in the modeling procedure owing to its high extensibility.

The two-dimensional analytical model of two different surface impedances arranged periodically and alternately in parallel is shown in Fig. 1. Boundary C_1 is formulated by the mode expansion method considering specular and scattering reflection components, and phantom region F_2 is formulated by BEM. In this structure, the excess attenuation is caused by its discontinuity of impedance, so that the normal incidence (incidence angle, $\theta = 0$) sound absorption coefficient α considering this excess attenuation is obtained by the following expression [17]:

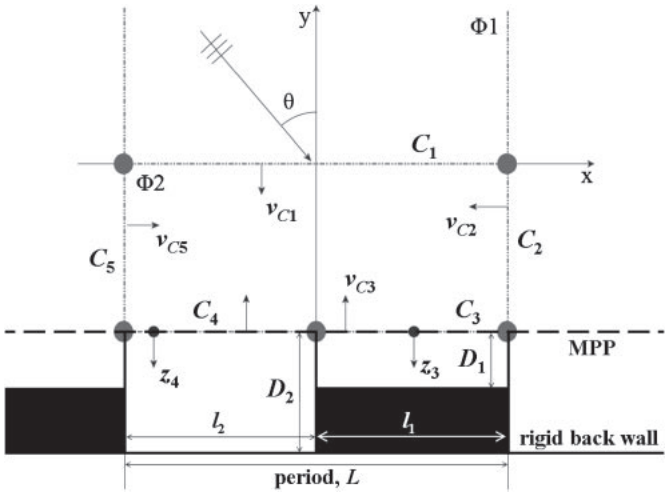

Fig. 1 Two-dimensional analytical model of hybrid boundary element method/mode expansion method. $V_{C1} \sim V_{C5}$: particle velocity direction, z_3 and z_4: normal impedances of boundaries C_3 and C_4.

$$\bar{\alpha} = 1 - \frac{1}{k_0 \cos\theta} \sum_{r=-\infty}^{\infty} |R_r|^2 \,\mathrm{Re}\left[\sqrt{k_0^2 - k_{x,r}^2}\right]. \tag{1}$$

Here, L is the period of the arrangement and k_0 is the acoustic wave number. $k_{x,r}$ is the rth mode reflection wave number (x direction), and R_r is the rth mode reflection coefficient on boundary C_1:

$$k_{x,r} = \frac{2\pi r}{L} + k_0 \sin\theta \tag{2}$$

$$R_r = u_r - \frac{1}{ik_{y,r}L} \sum_{j=1}^{N_{C1}} v_{C1,j} \int_{x_{j-1}}^{x_j} \exp(ik_{x,r}x)dx, \tag{3}$$

where

$$k_{y,r} = \begin{cases} \sqrt{k_0^2 - k_{x,r}^2}, & k_0^2 - k_{x,r}^2 \geq 0 \\ i\sqrt{k_{x,r}^2 - k_0^2}, & k_0^2 - k_{x,r}^2 < 0 \end{cases} \tag{4}$$

$$u_r = \begin{cases} 1, & r = 0 \\ 0, & r \neq 0 \end{cases}. \tag{5}$$

N_{C1} is the number of elements on boundary C_1, and $v_{C1,j}$ is the particle velocity of the jth component on boundary C_1. In the analysis, the following periodical conditions on boundaries C_2 and C_5 in region $\Phi 1$ are introduced:

$$\begin{bmatrix} p_{c5,j} = \exp(ik_0 L \sin\theta) p_{c2,j} \\ v_{c5,j} = -\exp(ik_0 L \sin\theta) v_{c2,j} \end{bmatrix}, \tag{6}$$

where $p_{C5,j}$ $p_{C2,j}$ and $v_{C5,j}$ $v_{C2,j}$ are the sound pressure and particle velocity of the jth component on each boundary. Locally reacting boundary conditions are also assumed, and $v_{C1,j}$ is formulated by BEM in this paper.

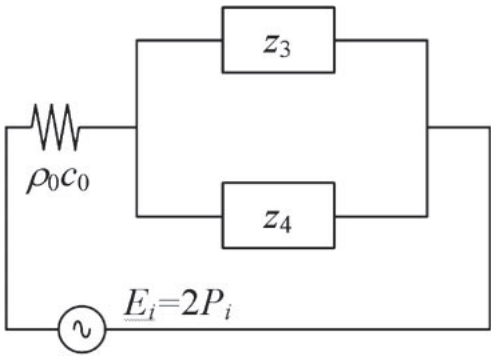

Fig. 2 Electro acoustical equivalent circuit. z_3 and z_4: normal impedances of boundaries C_3 and C_4.

2.2. Electro Acoustical Equivalent Circuit Model

When the period L is large relative to the acoustic wavelength, the average of the sound absorption coefficient $\bar{\alpha}$, over the entire surface is derived statistically as follows:

$$\bar{\alpha} = \frac{l_1}{l_1 + l_2}\alpha_3 \frac{l_2}{l_1 + l_2}\alpha_4 \tag{7}$$

$$\alpha_i = 1 - \left|\frac{z_i/\rho_0 c_0 - 1}{z_i/\rho_0 c_0 + 1}\right|^2 \quad i = 3, 4, \tag{8}$$

where ρ_0 is the air density and c_0 is the sound speed in air.

On the other hand, L is sufficiently small relative to the acoustic wavelength, and the impedance over the entire surface $\bar{z}$ is determined by its electro acoustical equivalent circuit (Fig. 2). In this case, the sound absorption coefficient over the entire surface $\bar{\alpha}$ is

$$\bar{\alpha} = 1 - \left|\frac{\bar{z}/\rho_0 c_0 - 1}{\bar{z}/\rho_0 c_0 + 1}\right|^2 \tag{9}$$

$$\bar{z} = \left[\frac{l_1}{l_1 + l_2}\frac{1}{z_3} + \frac{l_2}{l_1 + l_2}\frac{1}{z_4}\right]^{-1}. \tag{10}$$

2.3. Numerical Examples and Discussions

First, consider the sound absorption coefficient when the surface impedances $z_3 = \rho_0 c_0$ (complete absorption) and $z_4 = \infty$ (complete reflection) are given. Figure 3 shows the numerical results of the sound absorption characteristics calculated by Eq. (1) in comparison with the results calculated by Eqs. (7) and (9). The results are shown as a function of the non dimensional parameter $k_0 L$.

Regardless of the period L, the excess absorption characteristics indicate almost the same tendency: As $k_0 L$ becomes small, the excess absorption characteristics gradually become close to the absorption coefficient derived using the electro acoustical equivalent circuit. On the other hand, when $k_0 L$ is large, they are almost the same as the statistical average of the absorption coefficient. Such dips arise when the period has the following relationship

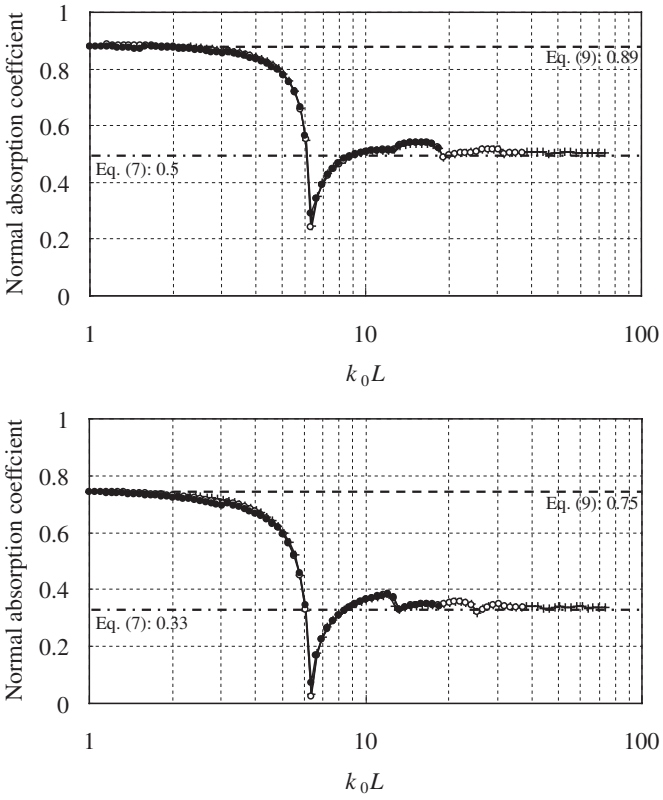

Fig. 3 Numerical results of sound absorption characteristics $\bar{\alpha}$ calculated by Eq. (1) (excess absorption) in the cases of $l_1 = l_2$ (top) and $2l_1 = l_2$ (bottom). The calculated results of Eqs. (7) and (9) are also shown in the same figures. The surface impedances are $z_3 = \rho_0 c_0$ (complete absorption) and $z_4 = \infty$ (complete reflection), respectively. Period $L = 1$ m (+), 0.5 m (○) and 0.25 m (●).

with the wave number of sound: $k_0 L = 2\pi$ ($L = \lambda$), where λ is the acoustic wavelength.

Next, consider the sound absorption coefficient when the surfaces have the acoustic impedances of MPP absorbers. The impedance of an MPP Z_H backed by an air back cavity and a rigid back wall is [2]

$$\frac{Z_H}{\rho_0 c_0} = \frac{8\eta l}{(d/2)^2}\sqrt{1 + \frac{R_{ey}^2}{32}} - i\omega\rho_0 l\left(1 + \sqrt{9 + \frac{R_{ey}^2}{2}}^{-1}\right) - i\sigma\cot(k_0 D_j) \quad j = 1, 2, \tag{11}$$

where d, σ and l are the hole diameter, perforation ratio, and thickness (= throat length) of an MPP, respectively. η is the coefficient of viscosity, ρ_0 is the air density, c_0 is the sound speed, and ω (= $2\pi f$; f is frequency) is the angular frequency of the sound. D is the air cavity depth and R_{ey} is the acoustical Reynolds number. The numerical examples are shown in Fig. 4. All the results of the excess absorption characteristics are higher than the statistical average of the absorption coefficient. When the period becomes smaller, the absorption peaks gradually become close to those

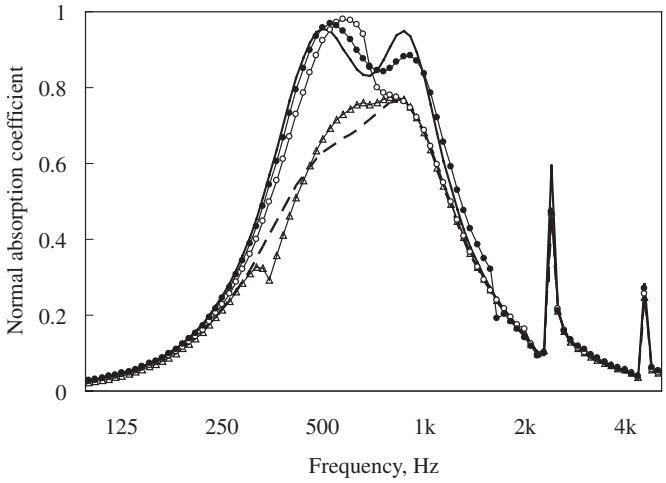

Fig. 4 Numerical results of sound absorption characteristics $\bar{\alpha}$ calculated by Eq. (1) (excess absorption) $L = 1$ m (△), 0.5 m (○) and 0.2 m (●), in comparison with Eqs. (6), solid, and (8), dashed. The surface impedances (see Figs. 1 and 2) are calculated by Eq. (10); hole diameter $d = 0.5$ mm, perforation ratio $\sigma = 1.23\%$, thickness (= throat length) $l = 1$ mm, and $D_1 = 50$ mm, $D_2 = 15$ mm.

derived using the electro acoustical equivalent circuit: the effect of excess absorption becomes more prominent with decreasing period. The result calculated using the equivalent circuit model is in best agreement with the smallest period. Therefore, the equivalent circuit analysis describes the ideal condition: the period is enough small for excess absorption.

Considering the circumstances described above, when $L > \lambda$, the excess attenuation does not arise under the normal incidence condition, and the sound absorption coefficient is in agreement with the statistical average of the absorption coefficient. On the contrary, when $L < \lambda$, the normal incidence sound absorption is mostly determined by the excess attenuation, and the absorption coefficient is in agreement with that derived using the electro acoustical equivalent circuit.

3. EXPERIMENT

3.1. Experimental Set Up

The normal incidence sound absorption coefficients were measured in accordance with ISO 10534-2 using

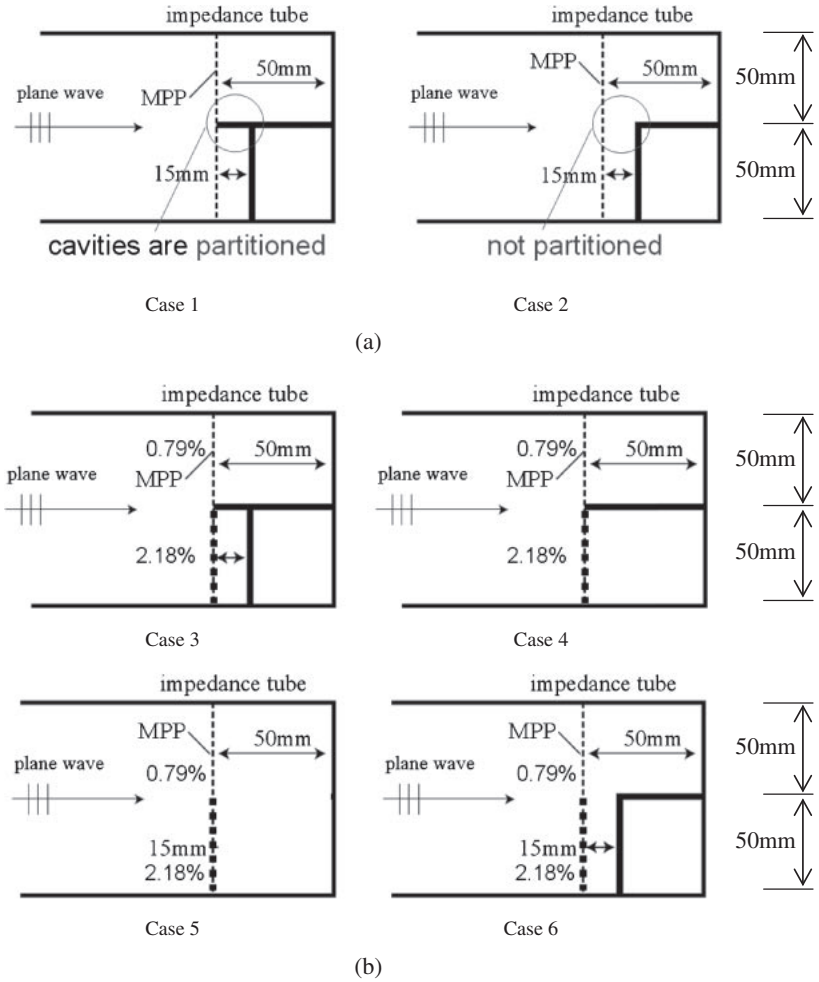

Fig. 5 Configurations of the specimens in an impedance tube. (a) Specimens using MPP1 with different cavity depths, (b) Specimens using MPP2 with different perforations and different cavity depths.

Table 1 Parameters of specimens used in the experiments.

	Material	Hole diamater mm	Thickness mm	Perforation ratio	Cavity depth mm
MPP1	metal	0.5	0.5	0.79	15/50
MPP2	polycarbonate	0.5	1	2.18/0.79	15/50

an impedance tube 100 mm diameter. Detail configurations of the specimens are described in Fig. 5. All the specimens are composed of two MPP absorbers with different frequency characteristics: one is a combination of different cavity depths, and the other is that of different perforation ratios. Each case has two patterns: the cavities are partitioned by an acrylic panel 5 mm thick in between, and cavities are not partitioned. Parameters of specimens used in the experiment are shown in Table 1.

3.2. Comparison with Electro Acoustical Equivalent Circuit Model

The experimental results are considered in comparison with the electro acoustical equivalent circuit model. The experimental results for the partitioned cavities are shown in Fig. 6. The sound absorption characteristics in all cases have two peaks and their frequencies correspond to the resonance frequencies in the uniform impedance. This phenomenon is obviously caused by a combination of two resonances. The absorption characteristics are larger than the statistical average of the absorption coefficient but in very good agreement with the values calculated using the equivalent circuit model.

On the other hand, the experimental results of the not partitioned cavities are shown in Fig. 7. In this case, however, in order to calculate the impedance over the entire surface $\bar{z}$, we must derive the MPP impedances from the measured data including the effect of the cavities. Therefore, the MPP impedances become (see also Fig. 8):

$$z_{MPP,j} = z_{meas,j} - i\cot(k_0 D_j) \quad j = 1, 2. \tag{12}$$

$\bar{z}$ determined using the equivalent circuit model when the cavities are not partitioned is

$$\bar{z} = 2\left[\frac{1}{z_{MPP,1}} + \frac{1}{z_{MPP,2}}\right]^{-1} + 2\left[\frac{1}{i\cot(k_0 D_1)} + \frac{1}{i\cot(k_0 D_2)}\right]^{-1}. \tag{13}$$

The measured sound absorption characteristics have only a peak caused by a single resonance and the absorption range does not broaden. The behaviors are in fairly good

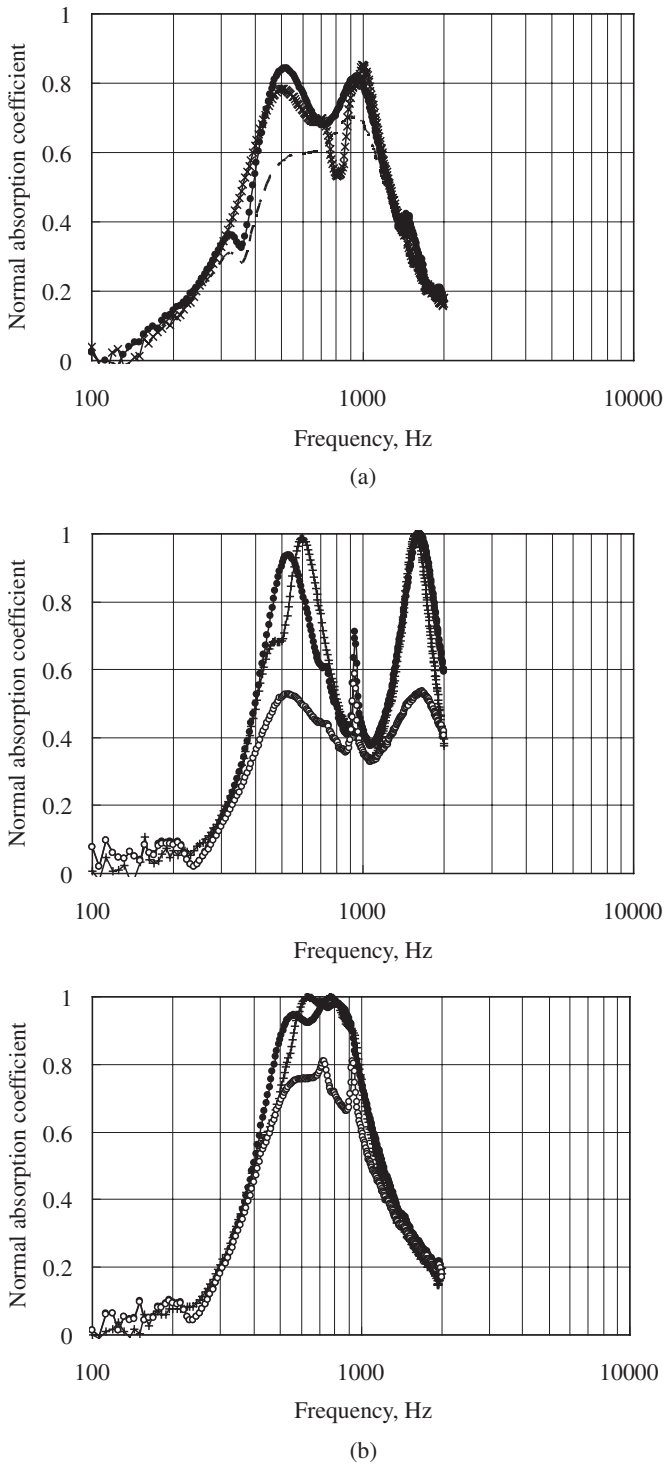

Fig. 6 Experimental results of the normal absorption coefficient. (a) Experimental results for Cases 1 (×) and 2 (solid), the average of the absorption coefficient (●) derived using the electro acoustical equivalent circuit, and the statistical average of the absorption coefficient (broken). (b) Experimental results (●) for Cases 3 (above) and 4 (below), the average of the absorption coefficient (+) derived using the electro acoustical equivalent circuit, and the statistical average of the absorption coefficient (○).

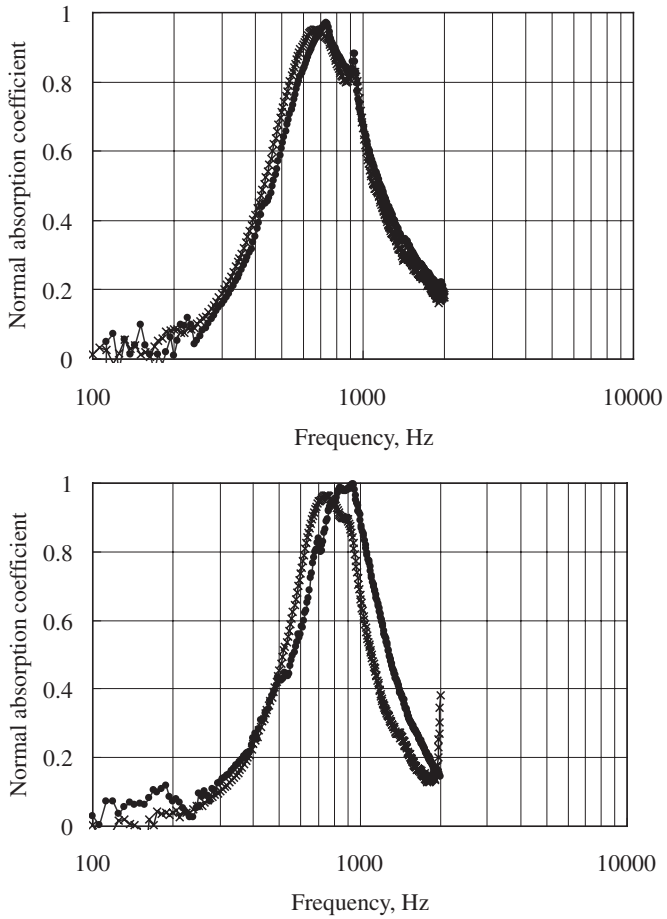

Fig. 7 Average of absorption coefficients derived using the electro acoustical equivalent circuit model (●) and measurement results (×) in Cases 5 (top) and 6 (bottom).

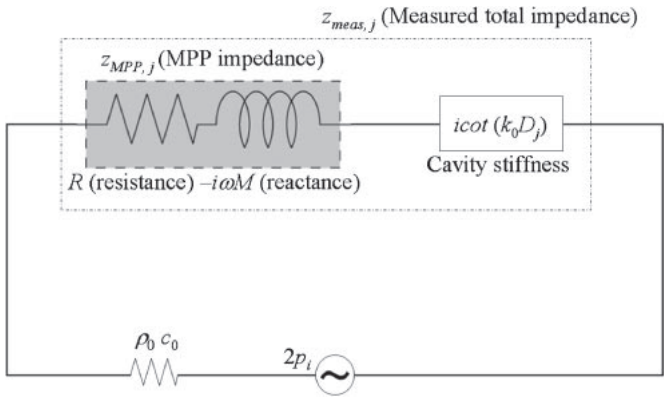

Fig. 8 Electro acoustical equivalent circuit model for the measured impedance of MPP in an impedance tube, including cavity stiffness.

agreement with the absorption coefficient derived using the equivalent circuit model. Therefore, the cavities should be partitioned in order to obtain wideband absorption characteristics effectively.

4. CONCLUDING REMARKS

The excess sound absorption characteristics of two microperforated panel absorbers with different impedances under the normal incidence condition have been analyzed by the Hybrid method of BEM and a mode expansion method, and the following was clarified. When the period is longer than the wavelength of sound, excess attenuation does not arise and the sound absorption coefficient is in agreement with the statistical average of the sound absorption coefficients of each absorber. On the contrary, when the period is shorter than the wavelength of sound, the normal incidence sound absorption is mostly determined by the excess attenuation, and the absorption coefficient is in agreement with the average values derived using the electro acoustical equivalent circuit model.

The electro acoustical equivalent circuit model was validated with experimental results: the average of the sound absorption coefficients derived using the electro-acoustical equivalent circuit model showed good agreement with the experimental results. The experimental results also showed that the cavities should be partitioned in order to obtain wideband absorption characteristics effectively.

REFERENCES

[1] D.-Y. Maa, "Theory and design of microperforated sound-absorbing constructions," *Sci. Sin.*, **17**, 55–71 (1975).
[2] D.-Y. Maa, "Microperforated-panel wideband absorber," *Noise Control Eng. J.*, **29**, 77–84 (1987).
[3] D.-Y. Maa, "Potential of microperforated panel absorber," *J. Acoust. Soc. Am.*, **104**, 2861–2866 (1998).
[4] H. V. Fuchs, X. Zha and H. D. Drotleff, "Creating low-noise environments in communication rooms," *Appl. Acoust.*, **62**, 1375–1396 (2001).
[5] X. Zha, H. V. Fuchs and H. D. Drotleff, "Improving the acoustic working conditions for musicians in small spaces," *Appl. Acoust.*, **63**, 203–331 (2002).
[6] M. Q. Wu, "Micro-perforated panels for duct silencing," *Noise Control Eng. J.*, **45**, 69–77 (1997).
[7] J. Kang and M. W. Brocklesby, "Feasibility of applying microperforated absorbers in acoustic window systems," *Appl. Acoust.*, **66**, 669–689 (2005).
[8] F. Asdrubali and G. Pispola, "Properties of transparent sound absorbing panels for use in noise barriers," *J. Acoust. Soc. Am.*, **121**, 214–221 (2007).
[9] J. Lee and G. W. Swenson, "Compact sound absorbers for low frequencies," *Noise Control Eng. J.*, **38**, 109–117 (1992).
[10] R. T. Randeberg, "Perforated panel absorbers with viscous energy dissipation enhanced by orifice design," Doctoral thesis, Norwegian Univ. (2000).
[11] K. Sakagami, M. Morimoto and W. Koike, "A numerical study of double-leaf microperforated panel absorbers," *Appl. Acoust.*, **67**, 609–619 (2006).
[12] K. Sakagami, T. Nakamori, M. Morimoto and M. Yairi, "Double-leaf microperforated panel space absorbers: A revised theory and detailed analysis," *Appl. Acoust.*, **70**, 703–709 (2009).

[13] M. Yairi, A. Minemura, K. Sakagami and M. Morimoto, "Effect of honeycomb structure in the back cavity on the absorption characteristics of microperforated panel absorbers," *J. Acoust. Soc. Am.*, **119**, 3250 (2006).
[14] M. Yairi and K. Sakagami, "Absorption characteristics of a microperforated panel absorber and increasing its absorption frequency range," *Proc. Spring Meet. Acoust. Soc. Jpn.*, pp. 1139–1142 (2010), (in Japanese).
[15] K. Sakagami, Y. Nagayama, M. Morimoto and M. Yairi, "Pilot study on wideband sound absorber obtained by combination of two different microperforated panel (MPP) absorbers," *Acoust. Sci. & Tech.*, **30**, 154–156 (2009).
[16] D. Takahashi, "Excess sound absorption due to periodically arranged absorptive materials," *J. Acoust. Soc. Am.*, **66**, 2215–2222 (1989).
[17] T. Fujimoto and K. Fujiwara, "Analysis of sound absorption by periodic structures using a hybrid-boundary element/mode expansion method," *Appl. Acoust.*, **64**, 525–532 (2003).